Charge-transfer fluctuation, d-wave superconductivity, and the B_{1g} Raman phonon in cuprates

T. P. Devereaux
Department of Physics, University of California, Davis, California 95616

A. Virosztek
Research Institute for Solid State Physics, POB 49, H-1525 Budapest, Hungary
and Institute of Physics, Technical University of Budapest, H-1521 Budapest, Hungary

A. Zawadowski
Institute of Physics, Technical University of Budapest, H-1521 Budapest, Hungary
and Research Institute for Solid State Physics, POB 49, H-1525 Budapest, Hungary
(Received 24 August 1994)

The Raman spectrum of the B_{1g} phonon in the superconducting cuprate materials is investigated theoretically in detail in both the normal and superconducting phases, and is contrasted with that of the A_{1g} phonon. A mechanism involving the charge-transfer fluctuation between the two oxygen ions in the CuO_2 plane coupled to the crystal field perpendicular to the plane is discussed and the resulting electron-phonon coupling is evaluated. Depending on the symmetry of the phonon, the weight of different parts of the Fermi surface in the coupling is different. This provides the opportunity to obtain information on the superconducting gap function at certain parts of the Fermi surface. The line shape of the phonon is then analyzed in detail both in the normal and superconducting states. The Fano line shape is calculated in the normal state and the change of the linewidth with temperature below T_c is investigated for a $d_{x^2-y^2}$ pairing symmetry. Excellent agreement is obtained for the B_{1g} phonon line shape in $YBa_2Cu_3O_7$.

I. INTRODUCTION

As a result of the recent dispute as to whether the superconducting gap in the high-T_c materials is s or d type, all experiments which can contribute to resolve that question are of special importance.[1] It was shown recently[2] that the study of the polarization dependence of electronic Raman scattering can address these questions and can distinguish between the different orientations ($d_{x^2-y^2}$ or d_{xy}) of the gap as well. This evidence can be made more complete by including phonons and the effect of the electron-phonon coupling, which is the subject of the present paper.[3]

The analysis of the line shape of optical phonons in the high-T_c superconductors has been the focus of a large body of investigation.[4,5] Of the many Raman-active modes in tetragonal superconductors, all the modes that have been observed in the cuprate materials using in-plane polarizations transform according the A_{1g} symmetry except one, which transforms according to B_{1g} symmetry.[5] Since this phonon obeys its own selection rules, the frequency of the mode can be unambiguously assigned, which is in contrast with the early confusion of the assignments of the separate A_{1g} modes.

In this paper the phonons involving the perpendicular vibrations of the in-plane oxygens are investigated. The displacements of the two oxygens O(2) and O(3) are in phase for A_{1g} symmetry and out of phase for B_{1g} as is shown on Fig. 1 for the case of $YBa_2Cu_3O_y$. The coupling of these phonons to the electrons in the plane has an interesting feature; namely, a completely flat CuO_2 plane taken out of the surrounding atomic environment has mirror symmetry through the plane. Thus the linear coupling between these phonons and the in-plane electrons is absent. In a crystal, however, as pointed out by

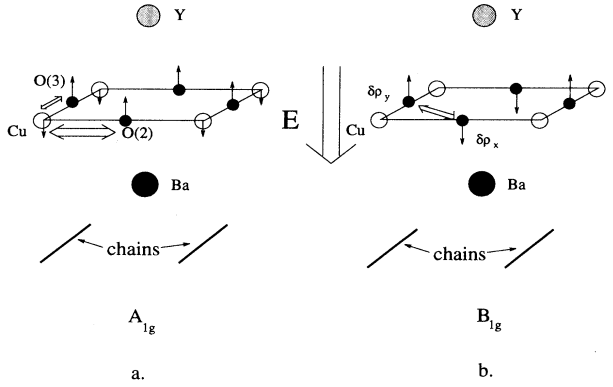

FIG. 1. The unit cell of the CuO_2 plane in $YBa_2Cu_3O_y$ is shown with the atomic displacements corresponding to the phonons of A_{1g} (a) and B_{1g} (b) symmetry. A finite electric field **E** perpendicular to the planes due to the asymmetric environment (Y above, Ba below) is indicated. This induces the respective charge-transfer fluctuations ($\delta\rho$) denoted by the two way arrows.

Barišić and Kupčić,[6] that symmetry can be broken since there is an electric field perpendicular to the plane due to the surrounding ions forming an asymmetric environment. This is in contrast to the La compound, where only the small tilting of the octahedra breaks the symmetry.[7] The perpendicular electric field in the 1:2:3 material can be responsible for the buckling of the CuO_2 plane, i.e., the slight separation of the planes formed by the Cu and O ions. This small distortion, however, cannot be responsible for the large electron-phonon coupling to be discussed here.

Since the long-range charge, transfer fluctuations between unit cells are screened, only intracell charge transfers must be considered. Let us denote the charge-transfer fluctuations at O(2) and O(3) by $\delta\rho_x$ and $\delta\rho_y$ (see Fig. 1), respectively. A charge-transfer fluctuation where $\delta\rho_x - \delta\rho_y \neq 0$ is obviously coupled to the electric field and the crystal deforms in the form of the B_{1g} phonon; similarly $\delta\rho_x + \delta\rho_y \neq 0$ is coupled to the A_{1g} phonon. The fluctuations of in-plane charges are either due to the transfer (i) between the in-plane oxygens and other ions, or (ii) between the two in-plane oxygens. The fluctuations of the A_{1g} symmetry $\delta\rho_x = \delta\rho_y$ can be a consequence of the transfers between the in-plane copper and oxygens. For B_{1g} symmetry both (i) and (ii) may be realized.

Considering the first possibility,[8] the charge transfer in 1:2:3 between the bridging oxygen O(4) and the O(3) is a good candidate. As long as the nonbonding orbital of O(4) parallel to the CuO chain has a partial electronic density of states near the Fermi surface, the transfer breaks x-y symmetry. That mechanism, which is sensitive to the position of the electronic partial density of states of the bridging oxygen relative to the Fermi energy, has been worked out in detail,[8] but the recently observed Raman spectra are not consistent with the predicted d_{xy} superconducting gap.[2]

The second possibility does not depend on such details of the electronic band structure, since only the conduction band plays a role. The charge-transfer fluctuation $\delta\rho_x + \delta\rho_y = 0$ between O(2) and O(3) involves especially those parts of the cylindrical Fermi surface which are close to the k_x and k_y axes. Thus the influence of the electron-phonon coupling on the electronic Raman continuum depends strongly on whether a large superconducting gap opens at that part of the Fermi surface. More precisely, the electronic contribution can be characterized by the azimuthal quantum number m on the cylindrical Fermi surface,[3,9] and $m = \pm 2$ corresponds to B_{1g} symmetry, while out of the two ($m = 0$, $m = \pm 4$) channels of A_{1g} symmetry only $m = \pm 4$ is relevant since the $m = 0$ mode describes charge fluctuations between cells, which are screened by the long-range Coulomb interaction. The different Fermi surface areas probed by Raman scattering in the A_{1g} and B_{1g} geometry are illustrated in Fig. 2. [A_{1g} and B_{1g} transforms like $\cos(4\phi)$ and $\cos(2\phi)$, respectively.] Thus assuming a $d_{x^2-y^2}$ type superconducting gap the B_{1g} mode probes the areas with the largest gap, while the A_{1g} averages the areas of both the largest gap and the nodes. The most appropriate tool in the Raman experiments to probe the electron-phonon coupling is to study the Fano interference which is formed due to the simultaneous scattering of light on the phonons and the electronic continuum (see, e.g., Refs. 4 and 8). The fit of the Fano line shape provides information not only on the coupling but also on the electronic continuum influenced by the opening of the superconducting gap. The appearance of a sharper gap in B_{1g} symmetry than in the A_{1g} provides a unique identification of the gap of $d_{x^2-y^2}$ type.[2] It must be emphasized, however, that these experiments are not sensitive to the sign of the order parameter and therefore cannot distinguish between d-wave superconductivity and a very highly anisotropic s type.

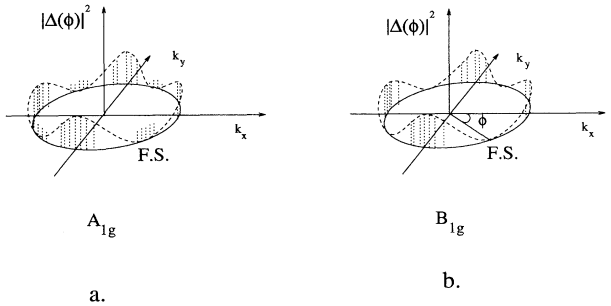

FIG. 2. The dashed line above the cylindrical Fermi surface (F.S.) represents a $d_{x^2-y^2}$ superconducting gap $|\Delta(\phi)|^2 \sim \cos^2(2\phi)$. The areas shaded by the vertical dotted lines mark the regions of the Fermi surface which are probed by Raman scattering in the A_{1g} (a) and in the B_{1g} (b) geometries.

The present status of the relation between experiment and theory can be summarized as follows. The vibration of the B_{1g} mode which appears at roughly 340 wave numbers in all cuprate materials is connected with the antisymmetric out-of-plane vibrations of the O(2) and O(3) ions in the Cu-O plane.[5] The net charge transfer of this vibration in the unit cell is zero and thus the long-range Coulomb forces are incapable of screening the charge fluctuations. Consequently, the mode has a large cross section for scattering incoming photons and thus appears in Raman experiments as a large sharp signal centered at frequency shifts corresponding to the energy of the mode. Due to the strength and unambiguous identification of the mode, the B_{1g} phonon has been lavished with attention.[5] In particular, the spectral line shape of the mode has been a subject of intense scrutiny both in the normal and superconducting states of the cuprates. In the normal state, the asymmetry of the line shape indicates strong mixing of the phonon with the electronic continuum and fits to a Breit-Wigner or Fano line shape have been made with great success.[4] This has usually led to the assertion that the electron-phonon coupling at least for this mode is large. However, no estimates of the coupling from a microscopic theory have been presented except for the theoretical suggestion by Barišić and Kupčić.[6] Further, the anomalous changes of the B_{1g} phonon as the material enters into the superconducting state have also been exhaustively documented.[4,5,10] The temperature dependences of the changes in the B_{1g} phonon's line shape have been used to help determine

the magnitude of the energy gap of the superconductor.[10] Recently, a theory of Raman scattering in d-wave superconductors has been presented,[2,3] and while the general features of the theory fit well with the experiment, no detailed fit of the line shape could be made without further knowledge of the mechanism and strength of the electron-phonon coupling.

In the present paper we provide a detailed theory for the behavior of the B_{1g} phonon in both the normal and superconducting states of the cuprate materials using the mechanism suggested by Barišić *et al.*[6,7] In particular, we investigate the mechanism of electron-phonon coupling resulting from crystal field effects and describe the Fano line shape in the normal state. The theory is then generalized to the superconducting state and the line shape is calculated in detail for a superconductor with $d_{x^2-y^2}$ pairing.

The paper is organized as follows. In Sec. II we develop the mechanism which leads to first-order electron-phonon coupling due to the presence of the crystal field. Based on the three-band model for the CuO_2 plane the electron-phonon coupling constant is evaluated. In Sec. III we apply these results in order to fit the experimental data in the normal state. Particular attention is paid to the Fano resonance. Section IV is devoted to the behavior of the phonon line shape in the superconducting state. Here we show that the temperature dependence of the spectrum is due to the change in the electronic response, and the data are consistent with a $d_{x^2-y^2}$ gap. Finally our conclusions are given in Sec. V.

II. MECHANISM

In the first part of this section we define our model for the electrons in the CuO_2 plane. This allows us to introduce notations used in the second part, where we develop a microscopic theory of the coupling of these electrons to the out-of-plane phonons due to the crystal field perpendicular to the plane.

A. Model

Using the notations of Ref. 11 we consider the three-band model for the CuO_2 plane described by the following Hamiltonian:

$$H^0=\varepsilon\sum_{\mathbf{n},\sigma}b^\dagger_{\mathbf{n},\sigma}b_{\mathbf{n},\sigma}+t\sum_{\mathbf{n},\boldsymbol{\delta},\sigma}P_{\boldsymbol{\delta}}(b^\dagger_{\mathbf{n},\sigma}a_{\mathbf{n},\boldsymbol{\delta},\sigma}+\text{H.c.}), \tag{1}$$

where $b^\dagger_{\mathbf{n},\sigma}$ creates an electron with spin σ at a copper lattice site $\mathbf{n}$, while $a_{\mathbf{n},\boldsymbol{\delta},\sigma}$ annihilates an electron at one of the neighboring oxygen sites $\mathbf{n}+\boldsymbol{\delta}/2$ determined by the unit vector $\boldsymbol{\delta}$ assuming the four values, $(\pm1,0)$ and $(0,\pm1)$. An oxygen atom between the two copper atoms at sites $\mathbf{n}$ and $\mathbf{n}+\boldsymbol{\delta}$ is labeled by either $(\mathbf{n},\boldsymbol{\delta})$ or $(\mathbf{n}+\boldsymbol{\delta},-\boldsymbol{\delta})$. Moreover, $\varepsilon=E_d-E_p$ is the difference of the Cu and O site energies, t is the Cu-O hopping integral, and $P_{\boldsymbol{\delta}}=\pm1$ depending on whether the orbitals (with real wave functions) have the same or opposite sign at the overlap region. Assuming Cu $d_{x^2-y^2}$ and O p orbitals $P_{-\boldsymbol{\delta}}=-P_{\boldsymbol{\delta}}$, and we can choose $P_{(1,0)}=1$ and $P_{(0,1)}=-1$. For simplicity, we neglect direct O-O hopping.

The momentum representation is defined by the following formulas:

$$b_{\mathbf{n},\sigma}=\frac{1}{\sqrt{N}}\sum_{\mathbf{k}}e^{i\mathbf{k}a\mathbf{n}}b_{\mathbf{k},\sigma} \tag{2}$$

and

$$a_{\mathbf{n},\boldsymbol{\delta},\sigma}=\frac{1}{\sqrt{N}}\sum_{\mathbf{k}}\exp[i\mathbf{k}a(\mathbf{n}+\boldsymbol{\delta}/2)]a_{\alpha,\mathbf{k},\sigma}, \tag{3}$$

where a is the lattice constant, N is the number of Cu sites, and α is x or y for $\boldsymbol{\delta}=(\pm1,0)$ and $\boldsymbol{\delta}=(0,\pm1)$, respectively. In this representation the Hamiltonian in Eq. (1) decouples for different momenta as

$$H^0=\sum_{\mathbf{k},\sigma}H^0_{\mathbf{k},\sigma}, \tag{4}$$

where

$$H^0_{\mathbf{k},\sigma}=\varepsilon b^\dagger_{\mathbf{k},\sigma}b_{\mathbf{k},\sigma}+\{ib^\dagger_{\mathbf{k},\sigma}[a_{x,\mathbf{k},\sigma}t_x(\mathbf{k})-a_{y,\mathbf{k},\sigma}t_y(\mathbf{k})]+\text{H.c.}\} \tag{5}$$

and

$$t_\alpha(\mathbf{k})=2t\sin(ak_\alpha/2). \tag{6}$$

$H^0_{\mathbf{k},\sigma}$ is then easily diagonalized as

$$H^0_{\mathbf{k},\sigma}=\sum_{\beta}E_\beta(\mathbf{k})d^\dagger_{\beta,\mathbf{k},\sigma}d_{\beta,\mathbf{k},\sigma}, \tag{7}$$

where β assumes the values $+$, $-$, and 0 for the antibonding, bonding, and nonbonding bands, respectively. The corresponding electronic energies are $E_0(\mathbf{k})=0$ and

$$E_\pm(\mathbf{k})=\varepsilon/2\pm\sqrt{(\varepsilon/2)^2+\Omega^2(\mathbf{k})}, \tag{8}$$

with

$$\Omega^2(\mathbf{k})=t_x^2(\mathbf{k})+t_y^2(\mathbf{k}). \tag{9}$$

The transformation between the original (a,b) and the new (d) electronic operators is described by

$$\begin{pmatrix}b\\a_x\\a_y\end{pmatrix}=(\mathbf{e}_+,\mathbf{e}_0,\mathbf{e}_-)\begin{pmatrix}d_+\\d_0\\d_-\end{pmatrix}, \tag{10}$$

where the column vectors of the transformation matrix are given by

$$\mathbf{e}_0=\frac{1}{\Omega}\begin{pmatrix}0\\t_y\\t_x\end{pmatrix} \tag{11}$$

and

$$\mathbf{e}_\pm=\frac{1}{\sqrt{E_\pm^2+\Omega^2}}\begin{pmatrix}E_\pm\\-it_x\\it_y\end{pmatrix}. \tag{12}$$

In the last three equations we have dropped the $\mathbf{k},\sigma$ in-

dices for clarity.

In the physically relevant situation for the CuO_2 plane the upper band is close to half filled. Since the three bands do not overlap in the present model, we will consider only a reduced one-band Hamiltonian describing the upper band and neglect the bonding and nonbonding bands. Then the reduced Hamiltonian is given by

$$H^0_{red} = \sum_{\mathbf{k},\sigma} E(\mathbf{k}) d^\dagger_{\mathbf{k},\sigma} d_{\mathbf{k},\sigma}, \tag{13}$$

with

$$E(\mathbf{k}) = \varepsilon/2 + \sqrt{(\varepsilon/2)^2 + \Omega^2(\mathbf{k})}. \tag{14}$$

Furthermore, the expressions of the transformation from d operators to a and b operators reduce to

$$b_{\mathbf{k},\sigma} = \phi_b(\mathbf{k}) d_{\mathbf{k},\sigma}, \tag{15a}$$

$$a_{x,\mathbf{k},\sigma} = \phi_x(\mathbf{k}) d_{\mathbf{k},\sigma}, \tag{15b}$$

$$a_{y,\mathbf{k},\sigma} = \phi_y(\mathbf{k}) d_{\mathbf{k},\sigma}, \tag{15c}$$

where

$$\phi_b(\mathbf{k}) = E(\mathbf{k})[E^2(\mathbf{k}) + \Omega^2(\mathbf{k})]^{-1/2}, \tag{16a}$$

$$\phi_x(\mathbf{k}) = -it_x(\mathbf{k})[E^2(\mathbf{k}) + \Omega^2(\mathbf{k})]^{-1/2}, \tag{16b}$$

$$\phi_y(\mathbf{k}) = it_y(\mathbf{k})[E^2(\mathbf{k}) + \Omega^2(\mathbf{k})]^{-1/2}. \tag{16c}$$

As we will see in the next subsection, this simple model contains the most important ingredients in order to describe the electron-phonon coupling.

B. Electron-phonon coupling

As we have discussed already, the electrons in the CuO_2 plane do not couple in first order to the phonon modes with displacement vectors perpendicular to the plane, because in that case the hopping integrals change only in second order in the displacements. However, if there is an electric field perpendicular to the plane, first-order electron-phonon coupling is generated. In our case this field originates from the asymmetric environment around the CuO_2 plane (see Fig. 1), and is also responsible for the buckling of the plane with restoring force provided by the covalent bonds.

Let us consider the effect of a lattice periodic crystal field $\mathbf{E}(\mathbf{r}) = -\nabla\phi_{ext}(\mathbf{r})$ on the electrons in the plane. The electron density at each (displaced) site couples to the external field via the Hamiltonian

$$\begin{aligned} H' = -e\sum_{\mathbf{n},\sigma}\{ & b^\dagger_{\mathbf{n},\sigma} b_{\mathbf{n},\sigma}\phi_{ext}[a\mathbf{n} + \mathbf{u}_b(a\mathbf{n})] \\ & + a^\dagger_{\mathbf{n},\mathbf{x},\sigma} a_{\mathbf{n},\mathbf{x},\sigma}\phi_{ext}[a\mathbf{n} + a\mathbf{x}/2 + \mathbf{u}_x(a\mathbf{n})] \\ & + a^\dagger_{\mathbf{n},\mathbf{y},\sigma} a_{\mathbf{n},\mathbf{y},\sigma}\phi_{ext}[a\mathbf{n} + a\mathbf{y}/2 + \mathbf{u}_y(a\mathbf{n})]\}, \end{aligned} \tag{17}$$

where $\mathbf{u}_b(a\mathbf{n})$, $\mathbf{u}_x(a\mathbf{n})$, and $\mathbf{u}_y(a\mathbf{n})$ are displacement vectors of the Cu, O(2), and O(3) in the unit cell at the lattice site $\mathbf{n}$, e is the electron charge, and $\mathbf{x}$ and $\mathbf{y}$ are unit vectors in the corresponding directions. Expansion in the displacements up to first order leads to

$$H' = H'_{\text{site}} + H_{\text{el-ph}} + \cdots, \tag{18}$$

where H'_{site} renormalizes the copper-oxygen site energy difference ε only, while the term linear in $\mathbf{u}$ generates an electron-phonon interaction

$$\begin{aligned} H_{\text{el-ph}} = e\sum_{\mathbf{n},\sigma}\{ & \mathbf{E}_b\mathbf{u}_b(a\mathbf{n}) b^\dagger_{\mathbf{n},\sigma} b_{\mathbf{n},\sigma} \\ & + \mathbf{E}_x\mathbf{u}_x(a\mathbf{n}) a^\dagger_{\mathbf{n},\mathbf{x},\sigma} a_{\mathbf{n},\mathbf{x},\sigma} \\ & + \mathbf{E}_y\mathbf{u}_y(a\mathbf{n}) a^\dagger_{\mathbf{n},\mathbf{y},\sigma} a_{\mathbf{n},\mathbf{y},\sigma}\}, \end{aligned} \tag{19}$$

where $\mathbf{E}_b$, $\mathbf{E}_x$, and $\mathbf{E}_y$ are the electric fields at the Cu, O(2), and O(3) sites, respectively, which are parallel to the z axis due to symmetry. In the absence of chains $\mathbf{E}_x = \mathbf{E}_y$ would hold.

$H_{\text{el-ph}}$ can be written in momentum representation with the help of Eqs. (2) and (3), and Eq. (15) allows us to express the interaction of phonons and electrons of the reduced Hamiltonian Eq. (13) in the usual form

$$H_{\text{el-ph}} = \frac{1}{\sqrt{N}}\sum_{\mathbf{q},\lambda}\sum_{\mathbf{k},\sigma} g_\lambda(\mathbf{k},\mathbf{q}) d^\dagger_{\mathbf{k}+\mathbf{q},\sigma} d_{\mathbf{k},\sigma}[c_\lambda(\mathbf{q}) + c^\dagger_\lambda(-\mathbf{q})]. \tag{20}$$

Here $c_\lambda(\mathbf{q})$ annihilates a phonon mode λ with wave vector $\mathbf{q}$ and $g_\lambda(\mathbf{k},\mathbf{q})$ is the coupling constant of that mode to an electron of wave vector $\mathbf{k}$. Based on our microscopic model the coupling constant can easily be evaluated using standard procedures of the quantum theory of phonons.[12]

In the context of Raman scattering we are interested in $\mathbf{q} = 0$ optical phonons. In case of the B_{1g} phonon the Cu displacement is zero, while the O(2) and O(3) atoms have equal and opposite displacements [Fig. 1(b)]. The corresponding coupling constant is evaluated as

$$\begin{aligned} g_{B_{1g}}(\mathbf{k},\mathbf{q}=0) = e\sqrt{\frac{\hbar}{2M_O\omega_{B_{1g}}}}\frac{1}{\sqrt{2}}[& (\mathbf{E}_x)_z|\phi_x(\mathbf{k})|^2 \\ & -(\mathbf{E}_y)_z|\phi_y(\mathbf{k})|^2], \end{aligned} \tag{21}$$

where M_O is the oxygen mass and $\omega_{B_{1g}}$ is the phonon frequency. In the following we make the approximation $(\mathbf{E}_x)_z = (\mathbf{E}_y)_z = E_z$. Due to the opposite displacements of the oxygens, the *difference* of the ϕ_α functions [given by Eq. (16)] determines the $\mathbf{k}$ dependence of the B_{1g} coupling. Since $\Omega(\mathbf{k}) = \text{const}$ on the Fermi surface [see Eq. (14)], this coupling constant is proportional to $t_x^2(\mathbf{k}) - t_y^2(\mathbf{k}) \propto \cos(ak_x) - \cos(ak_y)$, which is clearly of B_{1g} character. In fact, this is exactly the second-order Fermi surface harmonic[13] of our model band structure [Eq. (14)] transforming according to the B_{1g} symmetry. Therefore we can write the coupling in the form

$$g_{B_{1g}}(\mathbf{k},\mathbf{q}=0) = g_{B_{1g}}\phi^{m=2}_{B_{1g}}(\mathbf{k}), \tag{22}$$

where

$$\phi^{m=2}_{B_{1g}}(\mathbf{k}) = \frac{1}{\sqrt{N_{B_{1g}}(E_F)}}[\cos(ak_x) - \cos(ak_y)] \tag{23}$$

is the normalized second-order Fermi surface harmonic of B_{1g} symmetry with the normalization constant at the Fermi energy E_F given by[13]

$$N_{B_{1g}}(E_F) = \frac{\int d^2k\delta[E_F - E(\mathbf{k})][\cos(ak_x) - \cos(ak_y)]^2}{\int d^2k\delta[E_F - E(\mathbf{k})]}. \tag{24}$$

All information about the strength of the coupling is now compressed in the expansion coefficient

$$g_{B_{1g}} = -eE_z\sqrt{\frac{\hbar}{2M_O\omega_{B_{1g}}}}\frac{2t^2}{E_F(2E_F-\varepsilon)}\sqrt{\frac{N_{B_{1g}}(E_F)}{2}}. \tag{25}$$

In case of the A_{1g} phonon the oxygen displacements are the same both in magnitude and in direction [Fig. 1(a)] and the displacement of the copper is negligible due to the relative rigidity of its vertical bonds. The same procedure employed for the B_{1g} phonon yields the following coupling constant for the A_{1g} phonon,

$$g_{A_{1g}}(\mathbf{k}, \mathbf{q} = 0)$$

$$= eE_z\sqrt{\frac{\hbar}{2M_O\omega_{A_{1g}}}}\frac{1}{\sqrt{2}}[|\phi_x(\mathbf{k})|^2 + |\phi_y(\mathbf{k})|^2]. \tag{26}$$

In this case, however, the coupling depends on $\mathbf{k}$ only through the energy $E(\mathbf{k})$; i.e., it is constant on the Fermi surface for any band filling. Therefore within the present model the A_{1g} phonon couples to homogeneous density fluctuations only, and since these fluctuations are suppressed by the long-range Coulomb interaction, the resulting coupling is vanishingly small. This conclusion remains valid if we allow for a finite Cu displacement as well,[14] but does not necessarily hold if, e.g., O-O hopping is included.

At the end of this section we wish to evaluate the coupling in Eq. (25). For a half-filled band the Fermi energy $E_F = \varepsilon/2 + \sqrt{(\varepsilon/2)^2 + (2t)^2}$, and the normalization constant $N_{B_{1g}}(E_F) = 4$. It is reasonable to suppose that $\varepsilon/2 \ll 2t$, and in this limit we only need the electric field E_z at the oxygen site for a numerical value of $g_{B_{1g}}$. In order to estimate this field we suppose that the charges on the planes of the unit cell of $YBa_2Cu_3O_7$ are evenly distributed, and the charges (per unit cell, in units of e) for the planes Y, Ba, and CuO_2 are $+3$, $+2$, and -2 respectively, while the remaining (chain) region has -3 electron charge to ensure neutrality of the unit cell. Each plane produces an electric field at the oxygen site we are concerned with independent of its distance. Since all planes in the sample contribute, we consider ever larger environments of the CuO_2 plane in question. We calculate the field produced by the two neighboring (Y and Ba) planes first, then include the next nearest neighbors, etc. The series of values for E_z is of course not convergent, but has a period of the unit cell. Although a more accurate calculation applying the Ewald summation is desirable,[7] for an estimate we use the average value in this series, which yields $eE_z = -2\pi e^2/a^2 = -6.1$ eV/Å. According to Eq. (25) this crystal field generates a coupling $g_{B_{1g}} = 0.12$ eV. The relevant dimensionless coupling $\lambda_{B_{1g}} = N_F g^2_{B_{1g}}/\hbar\omega_{B_{1g}} = 0.078$ if we use a total density of states at the Fermi level $N_F = 0.22$/eV corresponding to a bandwidth of 9 eV. We note here that due to the presence of chains the tetragonal symmetry of the CuO_2 plane is weakly broken, and $(\mathbf{E}_x)_z \neq (\mathbf{E}_y)_z$. This leads to the slight mixing of the A_{1g} and B_{1g} modes.

III. NORMAL STATE

In this section we utilize our calculations for the coupling constant to discuss the resulting spectra of the cuprates in the normal state, while in the next section we discuss the changes in the spectra due to superconductivity.

The inelastic scattering of photons from a metal can either be caused by collisions with phonons or via the creation of electron-hole pairs. As well, the phonons interact with the electronic continuum and have a dynamical effect on the way photons are scattered. The total light scattering cross section resulting from these contributions is depicted by the Feynman diagrams in Fig. 3. The coupling constant γ describes the electron-photon coupling (i.e., the Raman vertex for particle-hole creation due to the vector potential of the incoming light). In the limit of small momentum transfer and frequency transfers smaller than the optical band gap, the Raman vertex is simply related to the curvature of the band dispersion $\epsilon(\mathbf{k})$ and the incident ($\hat{\mathbf{e}}^I$) and scattered ($\hat{\mathbf{e}}^S$) polarization light vectors via

$$\gamma(\mathbf{k}) = \frac{m}{\hbar^2}\sum_{\alpha,\beta} e^I_\alpha \frac{\partial^2\epsilon(\mathbf{k})}{\partial k_\alpha \partial k_\beta} e^S_\beta, \tag{27}$$

which can be expanded in terms of Fermi surface harmonics $\phi^m(\mathbf{k})$, $\gamma(\mathbf{k}) = \sum_m \gamma_m\phi^m(\mathbf{k})$. The remaining vertices we denote by $g_{p\text{-}p}$ for the photon-phonon vertex, and g_λ for the electron-phonon vertex as discussed in the previous section. The bare phonon propagator is given by

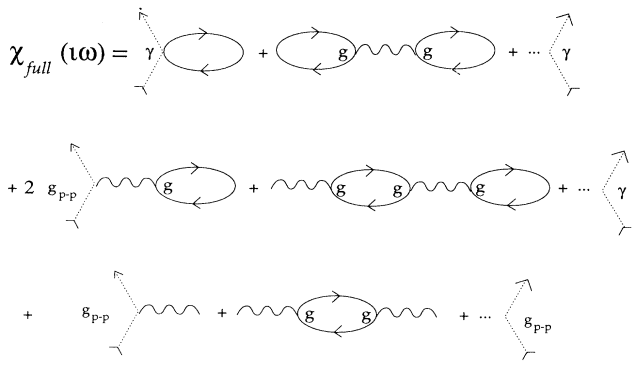

FIG. 3. Feynman diagrams depicting the three contributions to Raman scattering in metals. Here the solid line is the electron Green's function, the wavy line the phonon propagator, and the dashed line the photon propagator. The vertices are defined as in the text.

$$D^0_\lambda(\omega) = \frac{2\omega_\lambda}{\omega^2 - \omega^2_\lambda + 2i\omega_\lambda\Gamma^i_\lambda}, \tag{28}$$

where Γ^i_λ is the intrinsic phonon linewidth resulting from, e.g., the decay of the phonon caused by the presence of an anharmonic lattice potential. In the metallic state, the electron-phonon coupling renormalizes the phonon propagator such that

$$D_\lambda(\omega) = \frac{D^0_\lambda(\omega)}{1 + g^2_\lambda D^0_\lambda(\omega)\chi_\lambda(\omega)}, \tag{29}$$

where χ_λ is the complex electronic susceptibility evaluated in channel λ.[15] Defining the renormalized phonon frequency through

$$\hat{\omega}^2_\lambda = \omega^2_\lambda(1 - \lambda(\omega)), \tag{30}$$

where $\lambda(\omega) = 2g^2_\lambda\chi'_\lambda(\omega)/\omega_\lambda$ and χ' denotes the real part of the susceptibility, we arrive at the following expression for the renormalized phonon propagator:

$$D_\lambda(\omega) = \frac{2\omega_\lambda}{\omega^2 - \hat{\omega}^2_\lambda + 2i\omega_\lambda\Gamma_\lambda(\omega)}, \tag{31}$$

where Γ_λ is the total frequency-dependent linewidth of the phonon, $\Gamma_\lambda(\omega) = \Gamma^i_\lambda + g^2_\lambda\chi''_\lambda(\omega)$.

We now sum up the diagrams in Fig. 3 for the Raman response in terms of the susceptibility χ_λ. After some lengthy but trivial algebra we obtain

$$\chi''_{\lambda,\mathrm{full}}(\omega) = \frac{(\omega+\omega_a)^2}{(\omega^2 - \hat{\omega}^2_\lambda)^2 + [2\omega_\lambda\Gamma_\lambda(\omega)]^2}\left\{\gamma^2_\lambda\chi''_\lambda(\omega)\left[(\omega-\omega_a)^2 + 4\Gamma^i_\lambda\Gamma_\lambda(\omega)\left(\frac{\omega_\lambda}{\omega+\omega_a}\right)^2\right] + 4g^2_{p-p}\Gamma^i_\lambda\left(\frac{\omega_\lambda}{\omega+\omega_a}\right)^2[1+\lambda(\omega)/\beta]^2\right\}, \tag{32}$$

with

$$\beta = \frac{2g_{p-p}g_\lambda}{\gamma_\lambda\omega_\lambda}, \qquad \gamma_\lambda = \langle\phi_\lambda(\mathbf{k})\gamma(\mathbf{k})\rangle. \tag{33}$$

Here $\langle\cdots\rangle$ denotes an average over the Fermi surface. Thus γ_λ represents the symmetry elements of the Raman vertex projected out by the incoming and outgoing photon polarization vectors.

Equation (32) is a generalized form of the Breit-Wigner or Fano line shape describing the interaction of a discrete excitation (phonon) with an electronic continuum. Here the frequency $\omega_a = \omega_\lambda\sqrt{1+\beta}$ sets the position of the antiresonance of the line shape. If the intrinsic phonon width $\Gamma^i_\lambda = 0$, then at the antiresonance $\chi''_{\lambda,\mathrm{full}}(\omega = \omega_a) = 0$. Since χ_λ describes the electronic contribution to Raman scattering, which is generally featureless and a smooth function of frequency, we can replace everywhere χ_λ by the value it takes on near the phonon frequency to fit the Raman spectra in the vicinity of the phonon. However, to fit the entire spectrum in the normal state, the full ω dependence is required.

The description of the continuum in high-T_c superconductors has been the focus of a large body of both theoretical and experimental work. While at present no theory can completely describe the full symmetry-dependent continuum for a large range of frequency shifts, we now give expressions for the continuum in two separate cases. In the presence of impurity scattering, the continuum line shape has a simple Lorenztian form[16]

$$\chi''_\lambda(\omega) = N_F\frac{\omega\tau^{*-1}_\lambda}{\omega^2 + \tau^{*-2}_\lambda}. \tag{34}$$

Here $1/\tau^*_\lambda = 1/\tau_{m=0} - 1/\tau_\lambda$ is the channel-dependent impurity scattering rate reduced by vertex corrections. While this form can fit the data on the cuprate materials at least in the B_{1g} channel (i.e., crossed polarization orientations aligned 45° with respect to the a-b axis in the Cu-O planes) at low frequencies, the high-frequency tail which remains relatively constant and the frequency behavior at low frequencies in other channels cannot be accounted for.

Another form for the continuum can be arrived at by taking nesting of the Fermi surface into account as has been done by one of the present authors.[17] The Raman susceptibility has a similar form as Eq. (34) with the impurity scattering rate replaced by the addition of the electron-electron and impurity scattering rates on a nested Fermi surface and the effect of mass renormalization taken into account,

$$\tau^{*-1}_\lambda \to \tau^{*-1}_\lambda + \alpha\sqrt{(\beta'T)^2 + \omega^2},$$
$$\omega \to \omega m^*(\omega)/m,$$
$$\text{with } m^*(\omega)/m = 1 + \frac{2\alpha}{\pi}\ln\left[\frac{\omega_c}{\sqrt{(\beta'T)^2+\omega^2}}\right], \tag{35}$$

where α, β', and ω_c are constants determined by a fit to the electronic continuum in the normal state. This form for the Raman susceptibility provides an adequate description to the continuum in the normal state of both Y-Ba-Cu-O and Bi-Sr-Ca-Cu-O (see Ref. 17) and thus we will use this form rather than Eq. (34).

In order to fit the Raman spectra in the normal state, one sees from Eqs. (32) and (35) that a great deal of parameters are required. A fitting procedure is now discussed that greatly reduces the number of free parameters. The first step in the procedure is to determine the bare phonon parameters ω_λ and Γ^i_λ, which in princi-

ple can simply be read off from a fit to the line shape of the phonon in the insulating state where $g_\lambda = 0$. While the intrinsic width of the phonon can be read off as $\Gamma_\lambda^i = 2.5$ cm^{-1}, a problem arises with the position of the B_{1g} phonon, since it shows only a small renormalization with doping from the insulator to the metallic state,[18] the origin of which is unknown. This could be due in part to changes of the lattice parameters with doping and/or the tetragonal to orthorhombic transition.[5] Therefore, we thus must keep this parameter free and use the bare frequency we obtain from fitting the normal state. While in principle $g_{p\text{-}p}$ can be determined as well at this stage, since the intensity of the spectra is given in arbitrary units, this parameter (which sets the overall intensity) must also remain free.

Turning next to the metallic state, the continuum parameters α, β', and γ_λ are tuned to fit the full frequency range of the continuum minus the contribution of the phonons. We then tune the renormalized phonon position, $\hat{\omega}_{B_{1g}}$, which we later can compare with the result predicted from the value of $g_{B_{1g}}$ obtained in Sec. II. Thus the only unknown parameters are $g_{p\text{-}p}$ (and thus β), which also sets the antiresonance position ω_a, and the bare phonon frequency.

With these constraints, such a procedure produces the theory lines shown in Fig. 4(a) compared to the data of Ref. 19 on Y-Ba-Cu-O. The parameters used to obtain the fit are as follows: $\omega_{B_{1g}} = 358$ cm^{-1}, $\hat{\omega}_{B_{1g}} = 348$ cm^{-1}, $\Gamma_{B_{1g}} = 4.9$ cm^{-1}, $\Gamma^i_{B_{1g}} = 2.5$ cm^{-1}, $\alpha = 0.55$, $\beta' = 3.3$, $g^2_{B_{1g}} N_F/\omega_{B_{1g}} = 0.0624$, $\tau^{*-1}_{B_{1g}} = 600$ cm^{-1}, $\omega_c = 12\,000$ cm^{-1}, and $g_{p\text{-}p}/\gamma_{B_{1g}} = 0.0026$, which sets $\omega_a = 360$ cm^{-1}. Similar fits have been obtained before via the usual Fano expression[20,5] albeit with unconstrained parameters determined solely via a fitting routine. The value of the coupling constant used is roughly 20% smaller than the one given by the crude approximation in Sec. II. Given the uncertainty involved in the band parameters and the neglect of screening (which will reduce the crystal field and thus lower the coupling constant), we remark that the coupling constant derived from a microscopic picture of charge transfer within the unit cell provides an accurate description of the strength of the asymmetric Fano line shape of the B_{1g} phonon in Y-Ba-Cu-O.

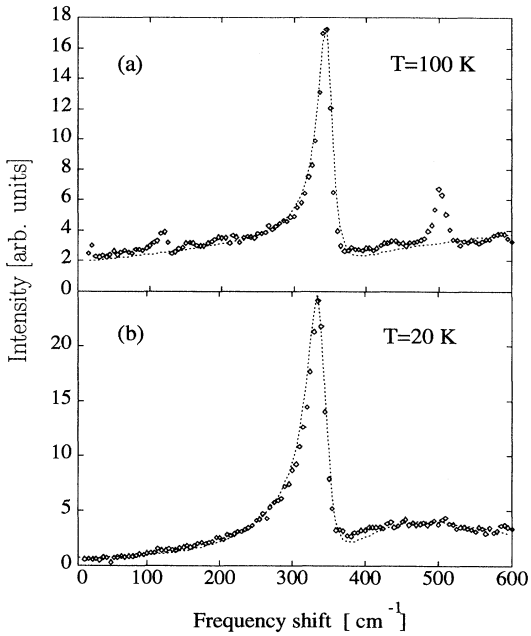

FIG. 4. (a) Fit of Eqs. (32), (34), and (35) to the B_{1g} spectra from Ref. 19 on Y-Ba-Cu-O at $T = 100$ K. The parameters used to obtain the fit are discussed in the text. (b) Fit of Eqs. (32) and (36) to the B_{1g} spectra from Ref. 21 on Y-Ba-Cu-O at $T = 20$ K. The parameters used to obtain the fit are discussed in the text. The additional phonons besides the 340 cm^{-1} have been subtracted off for clarity [see Fig. 4(a).

IV. SUPERCONDUCTING STATE

Turning now to the superconducting state, we note that Eq. (32) is still a valid description of the Raman line shape provided that we use the Raman susceptibility calculated for the superconducting case. In fact, it is possible to obtain important information about the symmetry of the electron pairing in a superconductor through an investigation of the changes in the phonon line shape below T_c. In particular, the electron-phonon coupling depends crucially on the symmetries of both the phonon and the order parameter. The role of the coupling between a phonon of given symmetry and an order parameter of a different symmetry was recently discussed by one of the authors,[3] where it was shown that changes in the phonon line shape are the greatest for a phonon which possesses the same symmetry as the order parameter while smaller changes are predicted for phonons of a symmetry orthogonal to that of the energy gap. This is pictorially shown in Fig. 2, which shows the energy gap $\Delta(\mathbf{k})$ squared and the electron-phonon vertex $g(\mathbf{k})$ squared, which enters into the Raman response function χ as a weighted average around the Fermi surface. Thus the phonon vertex and the energy gap will constructively (destructively) interfere with each other if they have the same (orthogonal) symmetry. This fact can be used to determine the predominant energy gap symmetry.

In Ref. 2 the electronic contribution to Raman scattering χ_λ was calculated in detail for a superconductor with $d_{x^2-y^2}$ pairing symmetry and good fits were obtained to the Raman spectra of Bi-Sr-Ca-Cu-O. For details of the theory, we direct the reader to that reference and simply write down the Raman response function obtained for the B_{1g} channel using a $d_{x^2-y^2}$ gap, $\Delta(\hat{\mathbf{k}}, T) = \Delta_0(T)\cos(2\varphi)$ for a cylindrical Fermi surface (here $x = \omega/\Delta_0$):

$$\chi''_{B_{1g}} = \tanh(\omega/4T)\frac{2N_F}{3\pi x}\begin{cases}[(2+x^2)K(x) - 2(1+x^2)E(x)], & x \le 1,\\ x[(1+2x^2)K(1/x) - 2(1+x^2)E(1/x)], & x > 1.\end{cases} \tag{36}$$

The real parts are obtainable through Kramers-Kronig analysis (see Ref. 3). The resulting response has a logarithmic divergence at the pair edge (an artifact of the two-dimensional nature of the Fermi surface) and vanishes as x^3 for small frequencies. To make a fit to the continuum in the superconducting state, we first convolute Eq. (36) with a Gaussian to mimic the effect of finite z dispersion of the Fermi surface, impurity effects, etc. Fitting the resulting function to the superconducting state continuum for Y-Ba-Cu-O leads to value $\Delta = 240$ cm^{-1} and a smearing width $\Gamma/\Delta = 0.2$ applied directly to $\chi''_{B_{1g}}$ (not to be confused with the intrinsic phonon linewidth). Then, Eq. (36) can be used to draw a fit to the full B_{1g} response using the parameters obtained from the fit to the response in the normal metal.

The resulting fit to the line shape using Eq. (36) and its corresponding real part (determined via Kramer's Kronig transformation) at $T = 20$ K is shown in Fig. 4(b) compared to the data on Y-Ba-Cu-O from Ref. 21. Here the parameters used are the same as in the normal metal case (Sec. III) with the only change resulting in the use of Eq. (36) and its real part rather than Eqs. (34) and (35). Using the coupling constant $\lambda = 0.0624$ as obtained in fitting the normal state leads to $\hat{\omega}_{B_{1g}} = 337$ cm^{-1} and $\Gamma_{B_{1g}} = 7.9$ cm^{-1}; i.e., the phonon broadens and softens at low temperatures compared to its normal state line shape.

The fit points towards the predominance of an energy gap of B_{1g} symmetry for the following reasons. First we remark that the theory predicts the correct magnitude and sign of the phonon renormalization due to superconductivity. This would be in marked contrast if the gap was s-wave or of d-wave nature but of other symmetry (d_{xy}, $d_{3z^2-r^2}$, etc.). In the first case an isotropic gap would lead to trivial coupling of the energy gap to the symmetry of the phonon and all phonons would show the same qualitative behavior, which is not the case for the cuprates.[5] In the second case, previous work has demonstrated that the channel probed via Raman scattering which shows a peak at the highest frequency in the continuum in the superconducting state of all the channels gives the predominant symmetry of the energy gap. This again points to $d_{x^2-y^2}$ pairing. Further, if the gap was of another symmetry (i.e., B_{2g} or A_{1g}), then the position of the phonon, $\omega_{B_{1g}}/\Delta = 1.42$, would predict small phonon softening since (i) the real part of the phonon self-energy changes from negative to positive values at roughly $\omega/\Delta = 1.5$, and (ii) the weight $\langle \gamma^2(\mathbf{k}) \mid \Delta(\mathbf{k}) \mid^2 \rangle$ over the Fermi surface which determines the coupling would be smaller for a gap of different symmetry than the vertex. Therefore, while although Raman cannot distinguish whether an energy gap changes sign or not around the Fermi surface, the evidence from the data indicate that the electronic pairing is predominantly of $d_{x^2-y^2}$ symmetry. As it will be discussed in Sec. V, it is very difficult to reconcile the data with even a strongly anisotropic s-wave gap.

V. CONCLUSIONS

In order to improve the study of the superconducting gap anisotropy in high-temperature superconductors[2,3] the interactions of the electronic continuum and the characteristic phonons shown in Fig. 1 have been included in the theory. These interactions and the intrinsic width of the phonons had complicated a previous comparison of the theory for the continuum for certain gap anisotropy to the experimental data since the contribution of the phonons had to be subtracted in an intuitive way (see Ref. 2). In addition, the phonon line shape is of course distorted by the Fano interference.

The starting point of our calculation was the model calculation of the electron-phonon interaction based on Ref. 6 and a simple tight-binding calculation for the electrons is used. The latter is certainly not very adequate but demonstrates the correct characteristic symmetry properties of the electronic wave functions.

Our main conclusions are as follows:

(i) *Phonon line shape.* The asymmetric Fano line shape of the B_{1g} phonon is reproduced while the interaction of the continuum with the A_{1g} phonon is much weaker according to the experiments[5] and disappears in our model calculation (see Sec. II B). Using more adequate electronic wave functions, this coupling may reappear but still must be weaker than in the case of the B_{1g} phonon.

(ii) *Electric field.* The perpendicular electric field acting on the oxygen atoms in the CuO_2 plane has been determined by a comparison with the experiments in the normal phase, assuming tetragonal symmetry, i.e., $\mathbf{E} = \mathbf{E}_x = \mathbf{E}_y$. This symmetry is certainly destroyed by the presence of the chains as shown in Fig. 1, and results in a mixing of the A_{1g} and B_{1g} symmetry channels. It is obvious from the coupling presented in Sec. II B and from the calculation of the diagrams depicting in Fig. 3 that starting with, e.g., light polarizations assigned to B_{1g} symmetry, the coupling with $\mathbf{E}_x \neq \mathbf{E}_y$ leads to a contribution to the electronic continuum of A_{1g} symmetry which is further coupled to the A_{1g} phonons. The A_{1g} phonons do appear in the B_{1g} spectrum observed by experiments [see Fig. 4(a)], but it is not clear whether this is dominantly due to misalignments of the samples or to the channel mixing. A more elaborate calculation of the electric fields $\mathbf{E}_x$ and $\mathbf{E}_y$ arising from different ions would certainly help to resolve this question.

(iii) *Gap anisotropy.* The excellent fit of the combined electronic continuum + phonon spectrum in Fig. 4(b) is obtained by assuming the simplest form of the superconducting gap of $d_{x^2-y^2}$ type for B_{1g} symmetry. The parameters are borrowed from the fitting of the normal state. The only additional parameters introduced are the gap amplitude defined above Eq. (36) and an additional smearing $\Gamma \sim 0.2\Delta_0$ with a nonunique origin (see Sec. IV). This fit certainly supports the previous fit in Ref. 2 where the phonons had been subtracted.

Concerning the anisotropy of the gap it has already been pointed out that Raman scattering provides information only concerning the absolute value of the gap. The fit of the low-energy spectra in the present paper clearly demonstrates that assuming d-wave pairing in the superconductor, the gap with $d_{x^2-y^2}$ symmetry gives an excellent fit but d_{xy}, d_{xz}, and d_{yz} are not applicable (see, e.g., Ref. 2). A very highly anisotropic extended s-wave state which has predominantly B_{1g} symmetry cannot be

ruled out.

For instance recently the photoemission experiment of Ref. 22 suggests a gap which can be represented by the form $\Delta(\varphi) = \Delta_0[1 + a\cos(4\varphi)]/(1 + a)$, with the parameter a just exceeding 1. Our fits clearly show that a fit with $a = 1$ are not satisfactory. The reason is that the different contributions of the different gap features to the low-energy ($\omega << \Delta_0$) part of the spectra with, e.g., B_{1g} symmetry: (i) The large gap around $\varphi = \frac{\pi}{2}n$ ($n = 0, 1, 2, \ldots$) does not contribute (see Fig. 2); (ii) the gap changing sign at $\varphi = \frac{\pi}{4} + n\frac{\pi}{2}$ contributes as ω^3 at low frequencies; (iii) the gap touching zero with zero slope (parameter $a = 1$) at $\varphi = \frac{\pi}{4} + n\frac{\pi}{2}$ contributes as ω at low frequencies (see Ref. 2); (iv) the gap with zero slope but not at zero energy (parameter $a \neq 1$) gives a sharp discontinuity and approximately linear term (modulo logs) above or below it ($a < 1$ and $a > 1$, respectively).

On the basis of the above features, the zero slope at energy larger than ~ 20 cm^{-1} and at $\varphi = \frac{\pi}{4} + n\frac{\pi}{2}$ can be ruled out. Any feature with a gap minimum on a smaller energy scale can, however, still be possible, but the region of the Fermi surface where the minima occur must be very narrow compared with those given by the expression mentioned above. As the minima should occur in an anomalously narrow region, the slopes coming or leaving the minima must be very large. Such a behavior appears to us as very unlikely.

In summary, the main result of the present paper is the confirmation of the conclusion of Refs. 2, 3, namely, that the Raman spectra are in excellent agreement with a superconducting gap of $d_{x^2-y^2}$ symmetry, but gaps with very sharp features on a small part of the Fermi surface cannot be ruled out.

Note added in proof. (1) It has been recently shown by one of us that the present work is not sensitive to the effect of impurity scattering [T. P. Devereaux (unpublished)]. Moreover, the analysis including impurity scattering provides further support for a gap of $d_{x^2-y^2}$ symmetry as opposed to highly anisotropic s-wave symmetry. (2) After completion of the manuscript, we became aware of the work by E. Rashba and E. Sherman [JETP Lett. **47**, 482 (1988)], in which the crystal field mechanism of the present paper was briefly discussed. Moreover, buckling as a source of electron-phonon coupling was examined in C. Thomsen *et al.*, Solid State Commun. **75**, 219 (1990). The resulting coupling is indeed significantly smaller than the one due to the crystal field, as it is pointed out in the Introduction.

ACKNOWLEDGMENTS

The authors would like to acknowledge stimulating discussions with G. T. Zimányi, B. Stadlober, D. Reznik, R. Hackl, J. C. Irwin, D. Einzel, and M. Cardona. One of the authors (T.P.D.) would like to acknowledge the hospitality of the Research Institute for Solid State Physics of the Hungarian Academy of Science and the Institute of Physics of the Technical University of Budapest where parts of this work were completed. This work was supported by the U.S.-Hungarian Science and Technology Joint Fund under Project No. 265, NSF Grant No. 92-06023, and by the Hungarian National Research Fund under Grants No. OTKA2950, 7283, and T4473.

[1] A. Sokol and D. Pines, Phys. Rev. Lett. **71**, 2813 (1993); S. Chakravarty, A. Sudbø, P. W. Anderson, and S. Strong, Science **251**, 337 (1993); N. Bulut, D. J. Scalapino, and S. R. White, Phys. Rev. B **47**, 6157 (1993).

[2] T. P. Devereaux *et al.*, Phys. Rev. Lett. **72**, 396 (1994).

[3] The effect of the electronic continuum on the phonons of different symmetry has recently been studied by T. P. Devereaux [Phys. Rev. B **50**, 10 287 (1994)] without using a definite model for the electron-phonon coupling and examining the Raman line shape.

[4] S. L. Cooper *et al.*, Phys. Rev. B **38**, 11 934 (1988).

[5] See, e.g., C. Thomsen, in *Light Scattering in Solids VI*, edited by M. Cardona and G. Güntherodt (Springer, Berlin, 1991). The role of interband scattering in the Raman efficiency [related to the anisotropy of $\gamma(\mathbf{k})$] was examined in T. Heyen *et al.*, Phys. Rev. Lett. **65**, 3048 (1990). The microscopic derivation of our phenomenologically introduced vertex, however, is far beyond the scope of the present paper.

[6] S. Barišić and I. Kupčić, in *High Temperature Superconductivity*, Vol. 23, *Strongly Correlated Electron Systems I*, edited by G. Baskaran, A. E. Ruckenstein, E. Tosatti, and Yu Lu (World Scientific, Singapore, 1990), p. 325.

[7] S. Barišić and I. Batistić, Europhys. Lett. **8**, 765 (1989).

[8] H. Monien and A. Zawadowski, Phys. Rev. Lett. **63**, 911 (1989).

[9] M. V. Klein and S. B. Dierker, Phys. Rev. B **29**, 4976 (1984); H. Monien and A. Zawadowski, *ibid.* **41**, 8798 (1990).

[10] V. G. Hadjiev *et al.*, Solid State Comm. **80**, 643 (1991).

[11] A. Zawadowski, Phys. Scr. T **27**, 66 (1989).

[12] See, e.g., N. W. Ashcroft and N. D. Mermin, *Solid State Physics* (Saunders College, Philadelphia, 1976), p. 780.

[13] P. B. Allen, Phys. Rev. B **13**, 1416 (1976).

[14] If the ratio of the copper and oxygen displacements of the A_{1g} mode is denoted by δ_{Cu}, we obtain instead of Eq. (26)

$$g_{A_{1g}}(\mathbf{k}, \mathbf{q} = 0) = eE_z\sqrt{\frac{\hbar}{2M_{\mathrm{O}}\omega_{A_{1g}}}}\frac{1}{\sqrt{2 + \delta_{\mathrm{Cu}}^2 M_{\mathrm{Cu}}/M_{\mathrm{O}}}} \times[|\phi_x(\mathbf{k})|^2 + |\phi_y(\mathbf{k})|^2 - \delta_{\mathrm{Cu}}|\phi_b(\mathbf{k})|^2(\mathbf{E}_b)_z/E_z].$$

Since $\phi_b(\mathbf{k}) = \text{const}$ on the Fermi surface [see Eq. (16a)], even the above more accurate expression does not yield significant (unscreened) coupling.

[15] More specifically,

$$\chi_\lambda(\mathbf{q}, i\omega) = \sum_{\mathbf{k},\mathbf{p}} \phi_\lambda(\mathbf{k})[i\omega\Phi_{\mathbf{k},\mathbf{p}}(\mathbf{q}, i\omega) + g(\mathbf{q})]\phi_\lambda(\mathbf{p}),$$

where ϕ_λ are Fermi surface harmonics in channel λ, Φ is the phase-space density Kubo function, and g is the wave-

vector-dependent compressibility, [see, e.g., D. Forster, *Hydrodynamic Fluctuations, Broken Symmetry, and Correlation Functions* (Benjamin, New York, 1975)].
[16]A. Zawadowski and M. Cardona, Phys. Rev. B **42**, 10 732 (1990).
[17]A. Virosztek and J. Ruvalds, Phys. Rev. B **45**, 347 (1992).
[18]D. Reznik *et al.*, Phys. Rev. B **48**, 7624 (1993).
[19]T. Staufer, R. Hackl, and P. Müller, Solid State Commun. **75**, 975 (1990); *ibid.* **79**, 409 (1991).
[20]G. Blumberg *et al.*, Supercond. **7**, 445 (1994), and references therein.
[21]R. Hackl *et al.*, Phys. Rev. B **38**, 7133 (1988).
[22]J. C. Campuzano *et al.* (private communication).